JAERI-M
84-088

DISTRIBUTION OF ^{60}Co AND ^{54}Mn IN GRAPHITE MATERIAL OF IRRADIATED HTGR FUEL ASSEMBLIES

May 1984

Kimio HAYASHI, Teruo KIKUCHI, Fumiaki KOBAYASHI,
Kazuo MINATO, Kousaku FUKUDA, Katsuichi IKAWA,
and Kazumi IWAMOTO

日本原子力研究所
Japan Atomic Energy Research Institute

JAERI-M レポートは，日本原子力研究所が不定期に公刊している研究報告書です。
入手の問合わせは，日本原子力研究所技術情報部情報資料課（〒319—11 茨城県那珂郡東海村）あて，お申しこしください。なお，このほかに財団法人原子力弘済会資料センター（〒319—11 茨城県那珂郡東海村日本原子力研究所内）で複写による実費頒布をおこなっております。

JAERI-M reports are issued irregularly.
Inquiries about availability of the reports should be addressed to Information Section, Division of Technical Information, Japan Atomic Energy Research Institute, Tokai-mura, Naka-gun, Ibaraki-ken 319—11, Japan.

編集兼発行　日本原子力研究所
印　　刷　日立高速印刷株式会社

JAERI-M 84-088

Distribution of ^{60}Co and ^{54}Mn in Graphite Material of Irradiated HTGR Fuel Assemblies

Kimio HAYASHI,[+] Teruo KIKUCHI,[++] Fumiaki KOBAYASHI, Kazuo MINATO, Kousaku FUKUDA, Katsuichi IKAWA and Kazumi IWAMOTO

Department of Fuels and Materials Research,
Tokai Research Establishment, JAERI

(Received April 18, 1984)

Distribution of ^{60}Co and ^{54}Mn was measured in the graphite sleeves and blocks of the third and fourth HTGR fuel assemblies irradiated in the Oarai Gas Loop-1 (OGL-1), which is a high temperature inpile gas loop installed in the Japan Materials Testing Reactor (JMTR) of Japan Atomic Energy Research Institute (JAERI). Axial and circumferential profiles were obtained by gamma spectrometry, and radial profiles by lathe sectioning with gamma spectrometry. Distribution of ^{60}Co is in good agreement with that of thermal neutron flux, and the Co content in the graphite is estimated to be $\sim 1 \times 10^{-9}$ in weight fraction. Concentration of ^{54}Mn decreases toward the axial center in its axial profile, and radially is almost uniform inside and appreciably higher at free surfaces. An estimated Fe content of $\sim 10^{-8}$ in wight fraction is smaller by two orders of magnitude than that from chemical analysis. Higher concentraion of ^{60}Co and ^{54}Mn at the free surfaces suggests the importance of transportation process of these nuclides in the coolant loop.

Keywords: Distribution, Profile, Cobalt-60, Manganese-54, Graphite, Activation Products, HTGR, Gamma Spectrometry, Impurity

---

+ Present address: OECD Halden Reactor Project, Halden, Norway.

++ Department of Research Reactor Operation, JAERI.

CONTENTS

目　　次

1. INTRODUCTION

In the design of high temperature gas-cooled reactor (HTGR) at Japan Atomic Energy Research Institute (JAERI), the fuel assembly consists of compacts, which are carbon powder consolidated body with dispersed coated fuel particles, and of graphite sleeve and block and other graphite materials.[1] In-pile experiments of the simulated HTGR fuel assembly have revealed various aspects of fuel behaviors, such as integrity of coated fuel particles and fuel compacts under realistic operation conditions,[2] and diffusion and release behavior of fission gases[3] and metal fission products.[4]

This paper describes an experimentally determined distribution of typical long-lived activation products of ^{60}Co and ^{54}Mn in the graphite materials of the third and fourth fuel assemblies irradiated in the Oarai Gas Loop No.1 (OGL-1), which is a high temperature in-pile gas loop installed in the Japan Materials Testing Reactor (JMTR) of JAERI.[5] Cobalt-60 is produced through a thermal-neutron absorption reaction of $^{59}Co(n,\gamma)^{60}Co$, and ^{54}Mn through a fast-neutron reaction of $^{54}Fe(n,p)^{54}Mn$. Distribution of these nuclides provides us with information on the impurity content of their target elements, and on the generation and transport process of the target and activated nuclides. In this paper the estimated impurity contents are compared with those for the previous experiments on the first and second OGL-1 fuel assemblies.[4] The work on the measured distribution of fission products will be published elsewhere.[6]

2. EXPERIMENTAL PROCEDURE

A schematic diagram of the third OGL-1 fuel assembly is shown in Fig.1. Only one rod is inserted into the graphite block for the third assembly, whereas three rods for the fourth assembly. Specification of these fuels is listed in Table 1. The structure of the fourth assembly is almost the same as of the first and second assemblies.[4]

The graphite material is IG-11 of Toyo Tanso,Co.Ltd., which is a fine-grained petroleum coke with a density of 1.78 Mg/m^3. The material has been graphitized at 3070K, and then purified by a fluoride gas at high temperature. The characteristics of this material are summarized in Table 2, and its impurity content determined by chemical analysis is listed in Table 3.

Irradiation condition of the third and fourth assemblies in the OGL-1 loop is also listed in Table 1. Figure 2 shows a typical temperature distribution calculated for the graphite sleeve and block of the third assembly. The maximum temperatures of the third and fourth fuel sleeves are 1410 and 1330K, respectively. The typical maximum temperature of the graphie block of the third assembly is 1080K.

After cooled for about three and two years for the third and fourth assemblies, respectively, the irradiated graphite was analyzed by gamma spectrometry with a high purity Ge detector. The experimental method to obtain the axial and radial profiles of the gamma emitting nuclides are the same as for the first and second assemblies.[4] In brief, the axial profile was measured by gamma spectrometry with a lead collimator slit, and the radial profile by lathe sectioning and gamma spectrometry of the graphite powder sample.

The circumferential distribution of the activity was measured by using short cylindrical sample of the graphite sleeve cut by 10 and 40 mm in length. The gamma rays through a lead collimator slit, whose width is 5 mm and whose path is normal to the sample cylinder axis, was analysed by the gamma spectrometer as the sample was rotated on its axis (see Fig.3).

The measured count rate of gamma rays from ^{60}Co and ^{54}Mn at the photoelectric peaks of 1332 and 834 keV, respectively, have been converted into their activity per unit weight of graphite, i.e. Bq/kg-graphite by making use of standard activity sources. These peaks were large enough for acquisition times (> 300 seconds) of the present experiment. The counting error due to the nuclear decay statistics is below several tens of percent, and small enough especially for activities larger than 10^5 Bq/kg-graphite.

Emphasis is placed on the relative, rather than absolute, distribution of ^{60}Co and ^{54}Mn in the present experiment. Therefore the counting efficiency has not been corrected precisely, especially for the geometrical shape factor and the self absorption effect of the sample in the axial profile measurement. In the radial measurement, however, the obtained absolute activity is sufficiently precise because of the small amount of the graphite powder sample, whose volume is less than 3×10^{-7} m^3 (0.3 cm^3) for the sleeve and less than 1.2×10^{-6} m^3 (1.2 cm^3) for the block.

3. RESULTS

3.1 Axial and Circumferential Distributions

Axial profiles of ^{60}Co and ^{54}Mn in the graphite sleeve and block are depicted in Fig. 4 for the third, and in Fig.5 for the fourth OGL-1 fuel assemblies.

The profiles of ^{60}Co in the sleeves and blocks of the both assemblies are essentially smooth curves, which gradually increases approximately toward the axial center. The curves are in good agreement with the axial distribution of thermal neutron flux of the JMTR around the OGL-1 loop. The same tendency on ^{60}Co profiles has been observed in all the three sleeves of the second fuel assembly.(4)

The concentration peak of ^{60}Co at 200 mm from the top of the third fuel sleeve (Fig.4) is ascribed to a high concentration spot occasionally made in a thermocouple hole, whose bottom is located between 200 and 210 mm from the sleeve top (see Fig.1 and Appendix).

The axial profile of ^{54}Mn in the sleeve shows a decreasing dendency toward the axial center in Figs. 4 and 5. This profile is similar to that of the same nuclide in the second fuel sleeve(4). The concentration peak of ^{54}Mn at 200 mm from the top is referred to the same cause as for ^{60}Co. On the other hand the profile of ^{54}Mn in the block is rather similar to that of ^{60}Co in the sleeves and blocks of both assemblies. It appears that the ^{54}Mn profile in the block reflects the axial distribution of fast neutron flux, which is similar to that of thermal neutron flux.

Circumferential distribution of ^{60}Co in the sleeve is almost flat at any axial position (Fig.6c), except at 200-210 mm from the top (Fig.6a; see Appendix).

3.2 Radial distribution

Radial profiles of ^{60}Co at different axial position of the graphite sleeve of the third fuel assembly is depicted in Fig.7. At any axial position the nuclide distributes uniformly all over the depth of the sleeve, except that it has an appreciably higher concentration at inner and outer surfaces.

Figure 8 shows the raidial profiles of ^{60}Co and ^{54}Mn in the graphite block of the third assembly. Cobalt-60 distributes almost in the same manner as in the sleeve: uniformly inside and with appreciably higher concentration at both surfaces.

The profile of ^{54}Mn is peculiar in the graphite block. It decreases by one to three orders of magnitude in accordance with the distance up to ~2 mm from the inner and outer surfaces. The concentration, however, increases with increasing depth from the free surfaces and eventually keeps a relatively constant value, which is comparable to the concentration at both surfaces. The high concentration region inside is almost exactly corresponding to the holes for the tie-rods and test specimens, which are made form Hastelloy X, a Ni based alloy containing Fe and other alloying elements. This fact suggests that the high concentration level of ^{54}Mn inside is due to the alloying element of Fe or its activated nuclide ^{54}Mn which transfered to the graphite surface during the irradiation.

In the graphite sleeve of the fourth assembly (Fig.9), ^{60}Co distributes in the same way as in the sleeve and block of the third assembly. The concentration of ^{54}Mn is also uniform inside and increases by one or two orders just below the inner and outer surfaces.

To sum up the measured results above, the concentration distribution of ^{60}Co is axially in good agreement with thermal neutron flux distribution of the reactor, and radially is uniform inside with appreciably higher value at the inner and outer surfaces. It is reasonable to consider that the neutron flux is uniform within the small area of the graphite sleeve and block of the fuel assembly, and that the ^{60}Co distribution except at the free surfaces should have reflected the thermal neutron flux profiles both axially and radially.

By contrast, the concentration of ^{54}Mn decreases toward the center in its axial profile, and radially is almost uniform inside (fourth assembly sleeve) but much higher at the free surfaces of the tierod holes and at the inner and outer surfaces of the fourth assembly.

4. ANALYSIS AND DISCUSSION

4.1 Estimation of Co content in graphite

Cobalt-60 is produced through a thermal-neutron absorption reaction of ^{59}Co (abundance 100%). The measured ^{60}Co distribution in the graphite sleeve and block except at their surfaces shows that we can reasonably assume that the ^{60}Co has been produced and accumulated inside the material directly in accordance with increasing thermal neutron fluence. On this assumption the content of ^{59}Co in the graphite is estimated by the following activation equation:

$$n_o = AG/10^3 FN_o \sigma \phi \sum_{j=1}^{n} (1-e^{-\lambda t_j})\ e^{-\lambda T_j} \qquad (1)$$

where n_o: content of impurity element in weight fraction

A: activity of the activation product (Bq/kg-graphite)

G: atomic number of target material

F: natural abundance of target material (weight fraction)

N_o: Avogadro's number (6×10^{23})

σ: average neutron cross section (m^2)

ϕ: average neutron flux $(m^{-2}s^{-1})$

λ: decay constant of the activation product (s^{-1})

n: number of irradiation cycle

t_j: irradiation time of j-th irradation cycle (s)

T_j: cooling time from the end of j-th irradiation cycle to the present (s)

and the factor 10^3 is used for conversion of unit.

The numerical values to be adopted in equation (1) and the estimated impurity content of Co are summarized in Tables 4 and 5. Only a concentration value in the radial profile is used here because of its higher reliability than in the axial profile in obtaining the absolute activity through comparison with measured standard source activity.

The estimated content of the impurity Co in the graphite is a weight fraction of $\sim 1 \times 10^{-9}$ ($\sim$1 ppb) both for the third and fourth assemblies. This value is almost the same as the content of $\sim 1 \times 10^{-9}$ for the second assembly[4], which was analysed in the same way. This impurity content should be reasonable for the highly purified graphite materials.

4.2 Estimation of Fe content in graphite

Manganese-54 is almost exclusively produced from iron through a fast neutron reaction $^{54}Fe(n,p)^{54}Mn$, where the natureal abundance of ^{54}Fe is 5.8 atomic percent.

The axial distribution of ^{54}Mn in the sleeve is rather peculiar, but radially it is comparatively flat except at the inner and outer surfaces. In estimating the content of Fe in the graphite, we adopt the following assumption: " below a certain depth from the free surfaces the generation process of Fe is described by a usual neutron activation equation, and its transportation into and out of the sleeve can be neglected."

The both radial and axial center position (390-400 mm from the top in Fig.9: 1×10^{4} Bq/kg-graphite) is chosen as the "bulk part" of the fourth fuel sleeve. The evaluation point for the third assembly is determined so that it corresponds to the dips between the tierod hole and the inner and outer surfaces in the radial profile (typically 5×10^{3} Bq/kg-graphite in Fig.8). The content of Fe estimated in the same way as above

is of the order of 10^{-8} in weight fraction of the graphite (Table 5). This is lower than the result from the chemical analysis (2.4×10^{-6} in Table 2) by two orders of magnitude. The considerably large difference suggests that the transportation process of ^{54}Mn and Fe should be taken into account in a more realistic evaluation of this impurity content.

4.3 Radioactivity and transportation behavior of ^{60}Co and ^{54}Mn

An activity level of 10^{6} Bq/kg-graphite (30μci/kg) for ^{60}Co is not so important in terms of activity inventory, compared with that of fission products. Cobalt-60 is, however, detected at every position of the OGL-1 loop by a fission-product plateout detection system.[7][8] Thus the contamination of primary circuit by ^{60}Co could be an important problem because of its long half life (5.26y) and high enegy gamma emission.

This is also the case with ^{54}Mn, which is detected in the loop by stronger activity than ^{60}Co. Manganese-54 appears to be deposited more easily onto the pipe of the loop and to behave in a complicated manner in the coolant loop.

Thus a proper treatment of the transportation process would be needed in a quantitative description of the distribution behavior of these nuclides.

5. CONCLUSIONS

(1) Concentration distribution of ^{60}Co in the graphite sleeve and block is axially in good agreement with thermal neutron flux profile, and radially uniform inside with appreciably higher values at the inner and outer surfaces.

(2) Content of Co in the graphite material is estimated to be a weight fraction of 1×10^{-9} both for the third and fourth OGL-1 fuel assemblies.

(3) Concentration of ^{54}Mn decreases toward the center of the sleeve in its axial profile, and is radially almost uniform inside but considerably higher at the inner and outer surfaces.

(4) A usual activation analysis gives an iron content of the order of 10^{-8} in weight fraction for the graphite material. This value is smaller by two orders of magnitude than that determined by chemical analysis.

(5) Higher concentration of ^{60}Co and ^{54}Mn at free surfaces suggests the importance of tranportation process of these niclides in a quantitative description of their behavior in the high temperature in-pile gas loop.

ACKNOWLEDGEMENTS

The authors are deeply indebted to members of JAERI who are kind enough to help us with the present work, especially to the staffs of Department of JMTR Project, and Hot Laboratory of Tokai Research Establishment.

5. CONCLUSIONS

(1) Concentration distribution of ^{60}Co in the graphite sleeve and block is axially in good agreement with thermal neutron flux profile, and radially uniform inside with appreciably higher values at the inner and outer surfaces.

(2) Content of Co in the graphite material is estimated to be a weight fraction of 1×10^{-9} both for the third and fourth OGL-1 fuel assemblies.

(3) Concentration of ^{54}Mn decreases toward the center of the sleeve in its axial profile, and is radially almost uniform inside but considerably higher at the inner and outer surfaces.

(4) A usual activation analysis gives an iron content of the order of 10^{-8} in weight fraction for the graphite material. This value is smaller by two orders of magnitude than that determined by chemical analysis.

(5) Higher concentration of ^{60}Co and ^{54}Mn at free surfaces suggests the importance of tranportation process of these niclides in a quantitative description of their behavior in the high temperature in-pile gas loop.

ACKNOWLEDGEMENTS

The authors are deeply indebted to members of JAERI who are kind enough to help us with the present work, especially to the staffs of Department of JMTR Project, and Hot Laboratory of Tokai Research Establishment.

REFERENCES

(1) e.g. YASUNO T. et.al.: JAERI-M 8399, p.6 (1979).

(2) IKAWA K. et.al.: JAERI-M 83-012, p.136 (1983).

(3) ibid., p.35.

(4) HAYASHI K.: J. Nucl.Materl., 116, 233 (1983).

(5) MATSUNAGA S. et.al.: Nihon-Genshiryoku-Gakkai Shi (J.At.Energy Soc. Japan) 21, 245 (1979).

(6) HAYASHI, K. et.al., to be submitted to J. Nucl. Mater. (1984).

(7) TERADA H., KATAGIRI M., TAKAHASHI H., WAKAYAMA N.: J. Nucl. Sci. Technol. 17, 225 (1980).

(8) TSUYUZAKI N.: private communication.

APPENDIX

A CONCENTRATION PEAK SPOT OF ^{60}Co AND ^{54}Mn IN THE GRAPHITE SLEEVE OF THE THIRD OGL-1 FUEL ASSEMBLY

It is noticed that the axial profile of ^{60}Co in the third fuel assembly has a distinctive peak at 200 - 210 mm from its top (Fig.4). This position corresponds to the bottom of a hole for a thermocouple inserted.

Figure 6a shows the as-irradiated circumferential distribution of ^{60}Co in the sliced graphite sleeve at this axial position; Fig.6b the ^{60}Co distribution in the same sample after enlarging the thermocouple hole from an original diameter 2 mm to 3 mm by drilling off its surface layer. The concentration peak at the thermocouple position has disappeared in Fig.6b, and the overall activity level has also decreased appreciably. It should be noted here that the true peak in Fig.6a is located at an angle of $(1/2)\pi$, and that the small peak at $(3/2)\pi$ is a deceptive peak observed from the opposite side of the cylindrical sample through the collimator slit.

The axial concentration peak of ^{54}Mn at $\sim$200 mm from the top corresponds to the ^{60}Co peak position.

On the basis of these facts the axial and circumferential peaks are ascribed to a spot of highly concentrated Co and Fe at the bottom of the thermocouple hole. The spot has been made presumably during fabrication process of the sleeve, for instance, because of Co and Fe which were contained in the drill for machining. Actually the sleeve has three holes for thermocouples. It appears that one of them occasionally carried the concentrated materials during machining.

Table 1 Specification and irradiation condition of fuel assemblies.

	3rd Fuels	4th Fuels
Number of Fuel Rod	three	one
Coated Fuel Particle	12% enriched U, UO_2 Kernel, TRISO Coating	19.9% enriched U, UO_2 Kernel, TRISO Coating
Fuel Compact *1	18^{ID} x 36^{OD} x 36^{L}	8^{ID} x 24^{OD} x 36^{L}
Graphite Sleeve *1	36.2^{ID}x46^{OD}x775^{L}	24.2^{ID}x30^{OD}x790^{L}
Graphite Block *1	50^{ID} x 80^{OD}x 780^{L}	80^{OD} x 785^{L} 32.6^{ID} x 3 holes *2
Graphite Inner Tube *1	13^{ID}x17.8^{OD}x730^{L}	
Irradiation Period	March 1979-July 1979	Nov.1979 - June 1980
Irradiation Time *3		
(hr)	976	1872
(s)	3.51×10^{6}	6.74×10^{6}
Maximum Burnup		
(% FIMA) *4	0.5	1.96
(MWD/T)	4.14×10^{3}	1.37×10^{4}
Maximum Fast Neutron Fluence ($m^{-2}s^{-1}$) (E>0.18MeV)	8.7×10^{23}	2.9×10^{24}
Maximum Outlet He Gas Temperature (K)	1200	1200

*1 Dimension in mm.

*2 Each hole is 32.6 mm in diameter (3 fuel rod).

*3 Effective full power time.

*4 Percentage of fissions per initial metallic atoms.

Table 2 Characteristics of graphite material.

	3rd OGL-1	4th OGL-1
Volume Density (Mg/m^3: g/cm^3)	1.78±0.02	1.78±0.01
True Density (Mg/m^3: g/cm^3)	2.16+0.01	2.15±0.01
Thermal Expansion Coefficient ($10^{-6}/K$)	4.54±0.13	2.15±0.01
Electric Resistance ($\mu\Omega m$)	11.3±0.7	10.8±0.6
Lattice Parameter (nm)	0.674±0.001	0.673±0.001

Table 3 Impurity content of graphite material obtained by chemical analysis.

Impurity Element	Impurity Content (weight ppm) 3rd OGL-1 Fuel	4th OGL-1 Fuel
Ag	ND *1	
Al	< 1.0	
B	< 100	0.6
Ca	< 0.5	2.7
Cd	ND	
Co	ND	
Cr	< 1.0	
Fe	< 50	2.4
Mg	< 50	0.47
Mo	ND	
Ni	< 10	
S	< 50	
Si	< 50	9.9
Ti	< 10	0.61
V	< 5	0.39
Dy+Eu+Ga+Sm	< 1 (ND)	
Ash	< 20	9 ± 1

*1 Not Detected.

Table 4 Numerical values for evaluation of impurity content of Co and Fe in the graphite material.

Abundance of ^{59}Co	1.0
Abundance of ^{54}Fe	0.058
Absorption Cross Section of ^{60}Co by Thermal Neutrons *1	2.2×10^{-27} m^2 (22b)
Cross Section of (n,p) Reaction of ^{54}Fe by Fast Neutrons (E>1MeV)	5.85×10^{-30} m^2 (58.5mb)
Maximum Thermal Neutron Flux (Along Axial Direction)	4.5×10^{17} $m^{-2}s^{-1}$
Fast Neutron Flux at The Evaluation Point (E>1MEV) *2	2×10^{17} $m^{-2}s^{-1}$
Half Life of ^{60}Co	1.66×10^{8} s (5.26y)
Half Life of ^{54}Mn	2.72×10^{7} s (303d)

*1 Spescific value averaged over the neutron spectrum for the OGL-1 fuel assembly.

*2 The value after the second OGL-1 fuel assembly.

Table 5 Estimated content of Co and Fe in graphite material.

		Activity (Bq/kg-graphite)	Impurity Content (wt. fraction)
Co	3rd Sleeve	1.2×10^{6}	1.2×10^{-9}
	3rd Block	1.2×10^{6}	1.2×10^{-9}
	4th Sleeve	2.0×10^{6}	1.0×10^{-9}
Fe	3rd Block	5×10^{3}	8×10^{-8}
	4th sleeve	1×10^{4}	4×10^{-8}

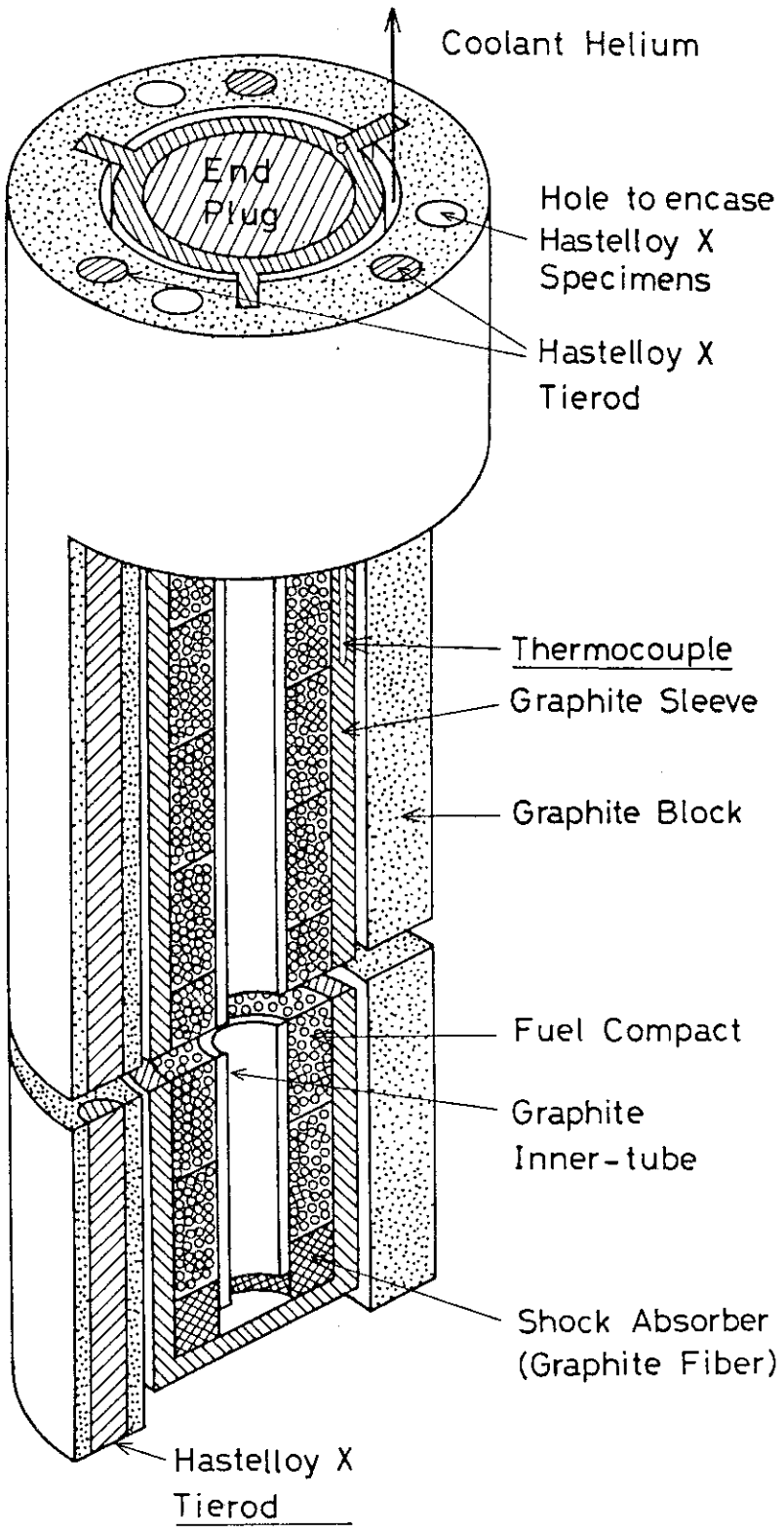

Fig.1 Schematic diagram of the third OGL-1 fuel assembly.

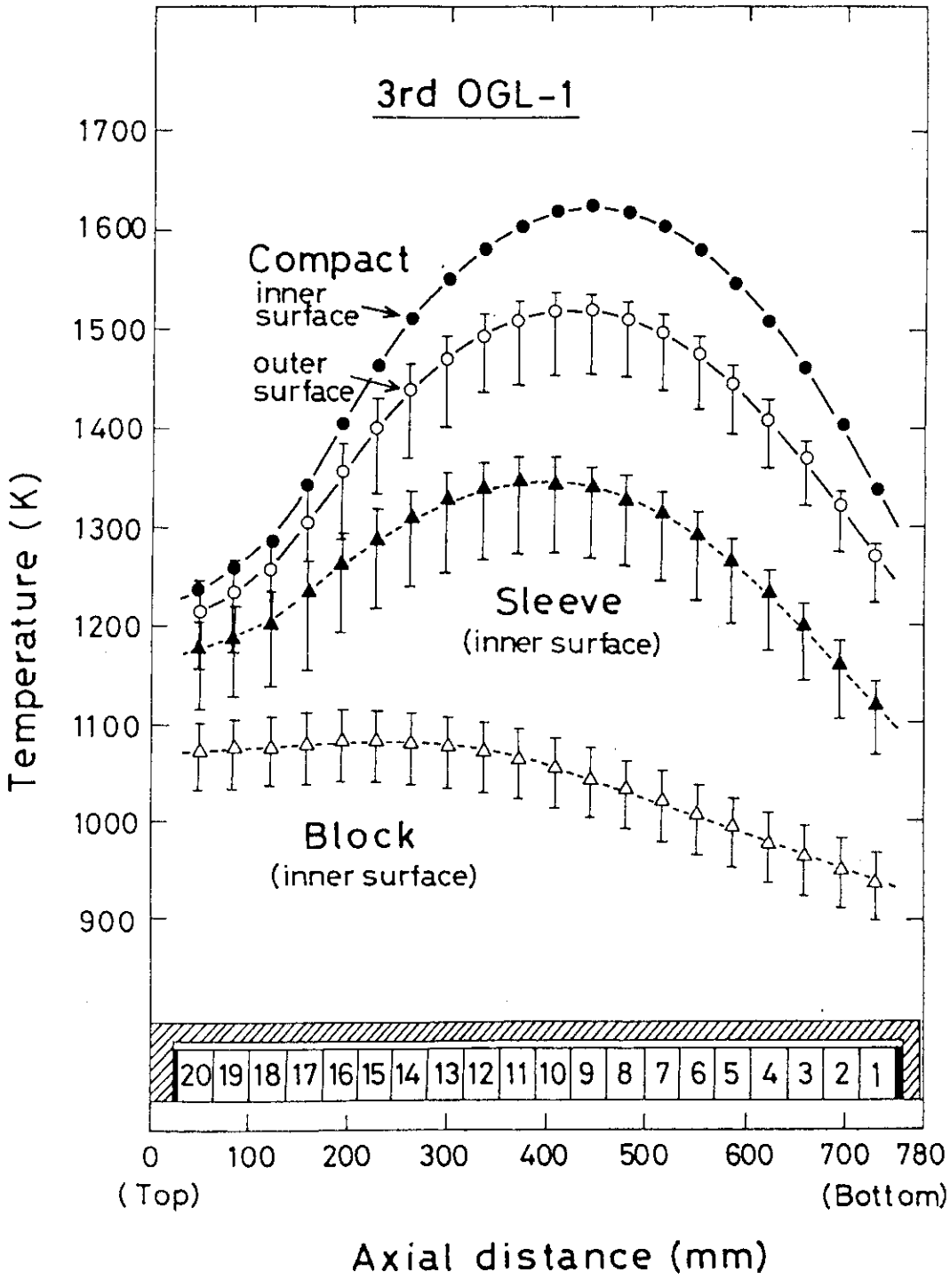

Fig.2 Typical temperature distribution of the third OGL-1 fuel assembly calculated for the latter half of the 46th cycle of the JMTR operation.

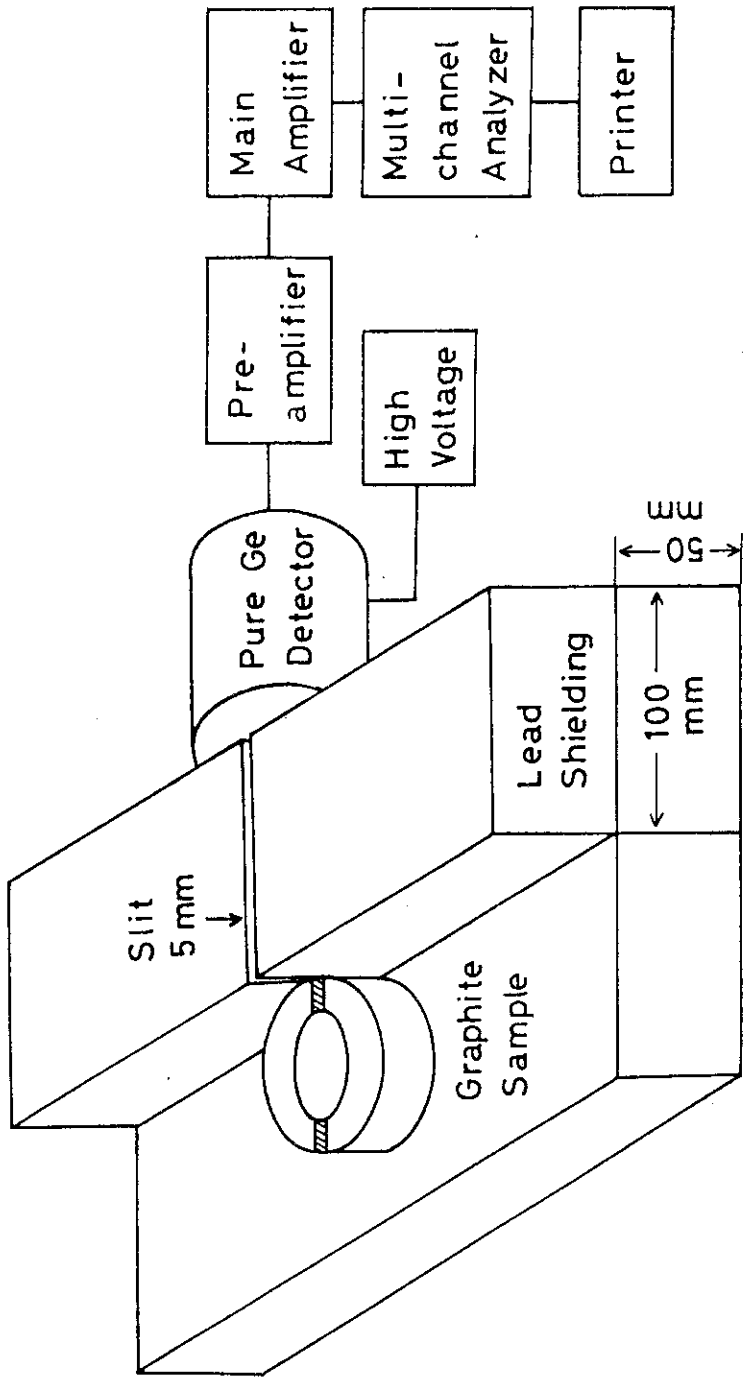

Fig.3 Schematics of circumferential distribution measurement of ^{60}Co and ^{54}Mn in the third OGL-1 graphite sleeve.

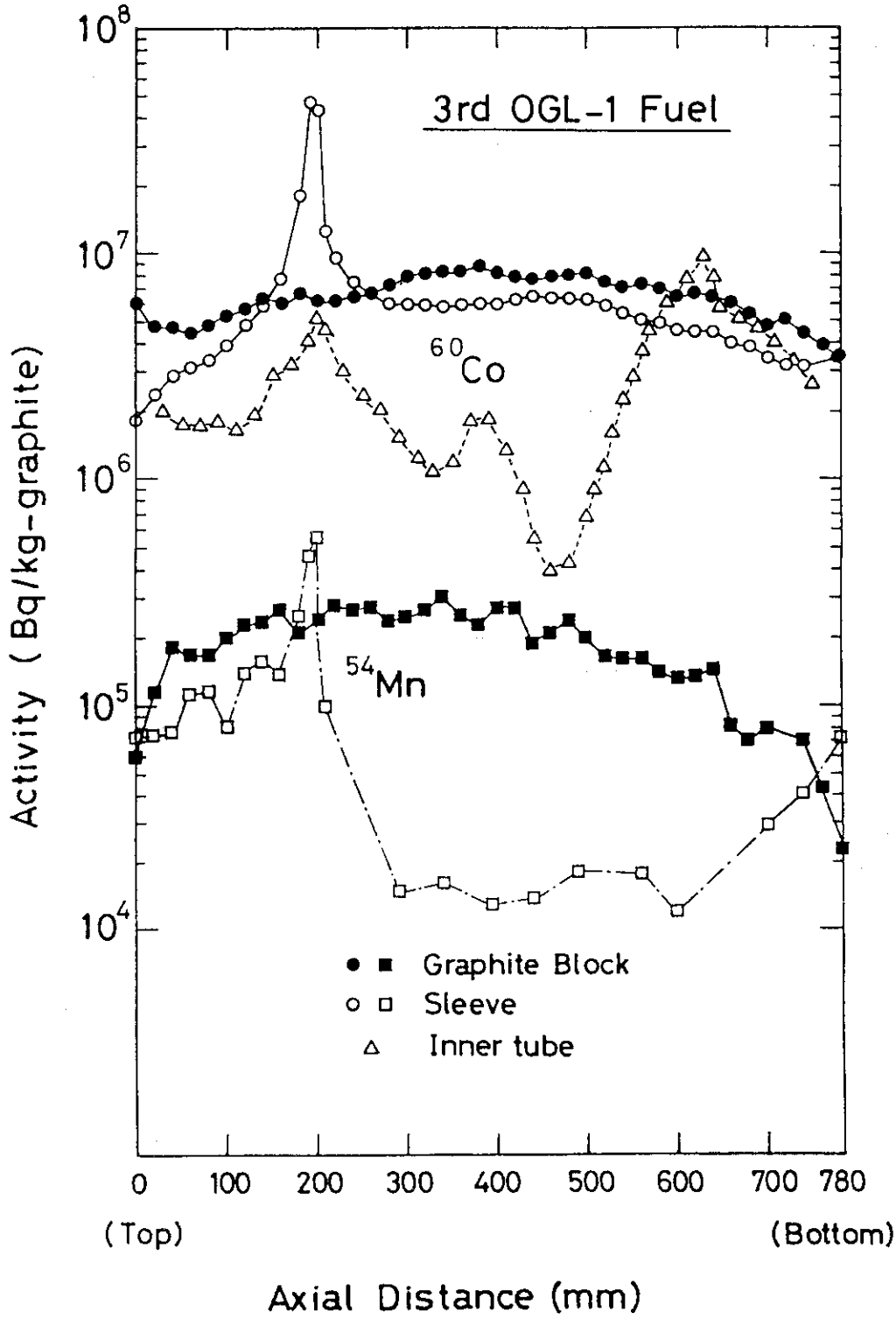

Fig.4 Axial profiles of ^{60}Co and ^{54}Mn in the third OGL-1 fuel assembly.

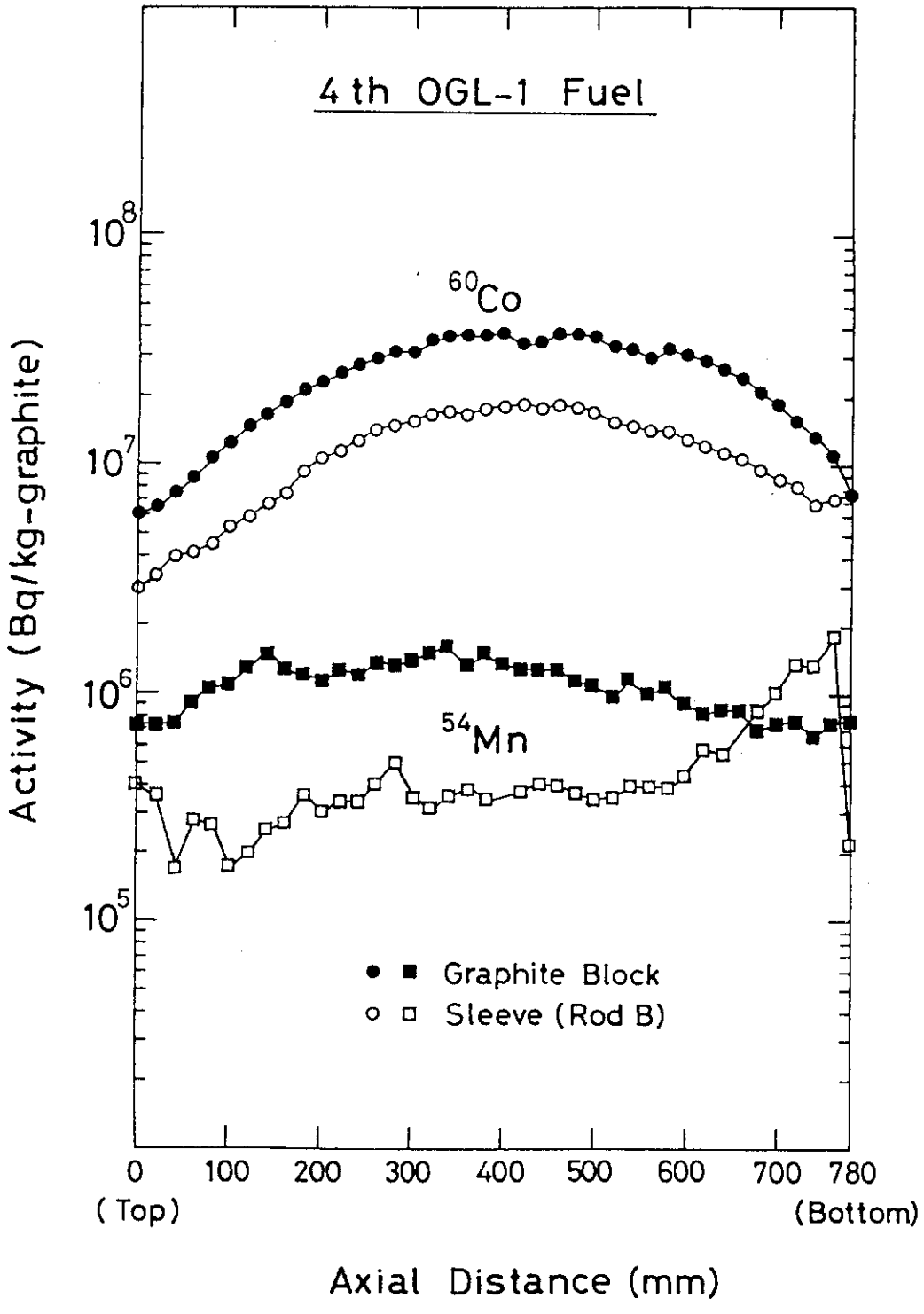

Fig.5 Axial profiles of ^{60}Co and ^{54}Mn in the graphite sleeve (rod B) and graphite block of the fourth OGL-1 fuel assembly.

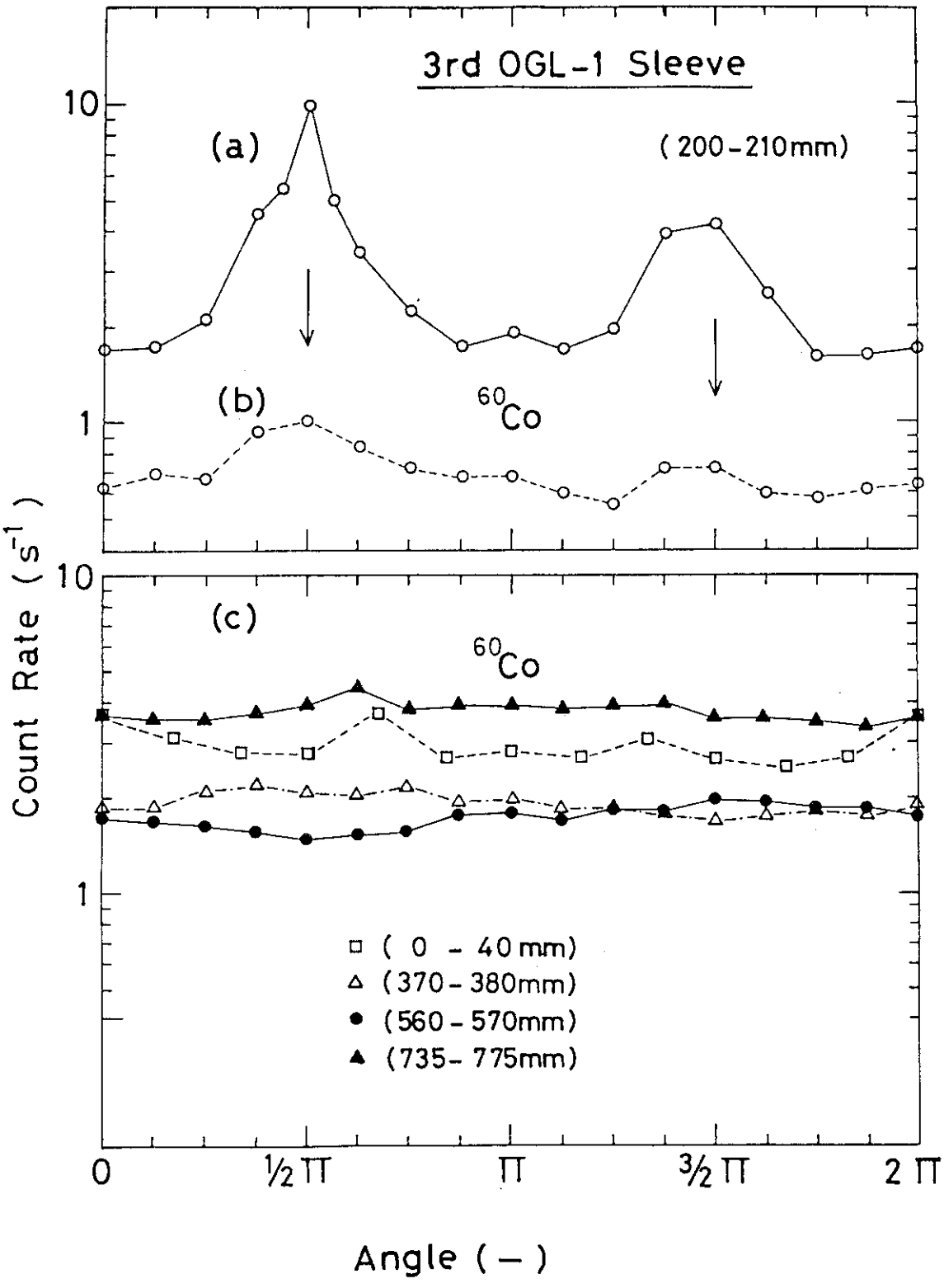

Fig.6 Circumferential distribution of ^{60}Co and ^{54}Mn in the third OGL-1 fuel sleeve.

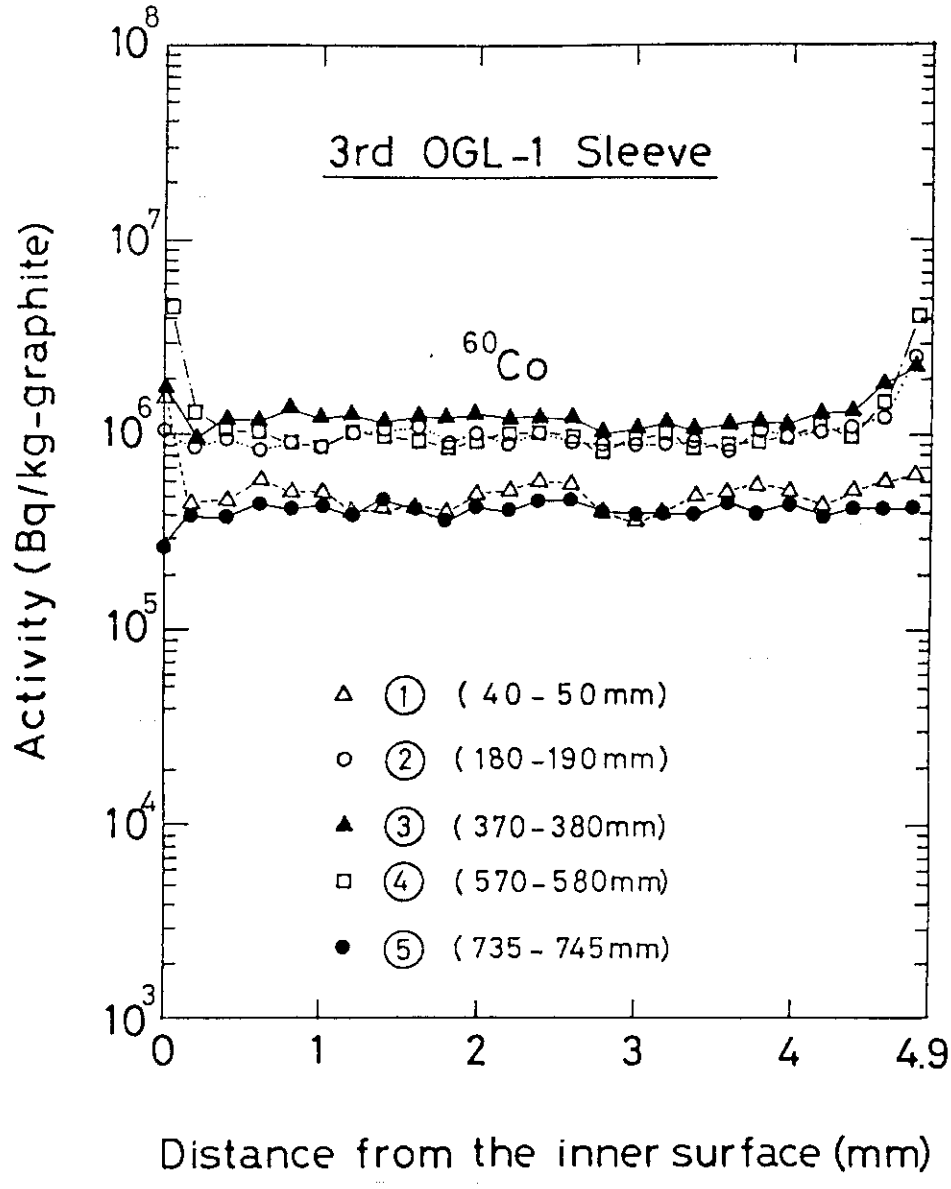

Fig.7 Radial profiles of ^{60}Co at different axial positions of the third OGL-1 fuel sleeve.

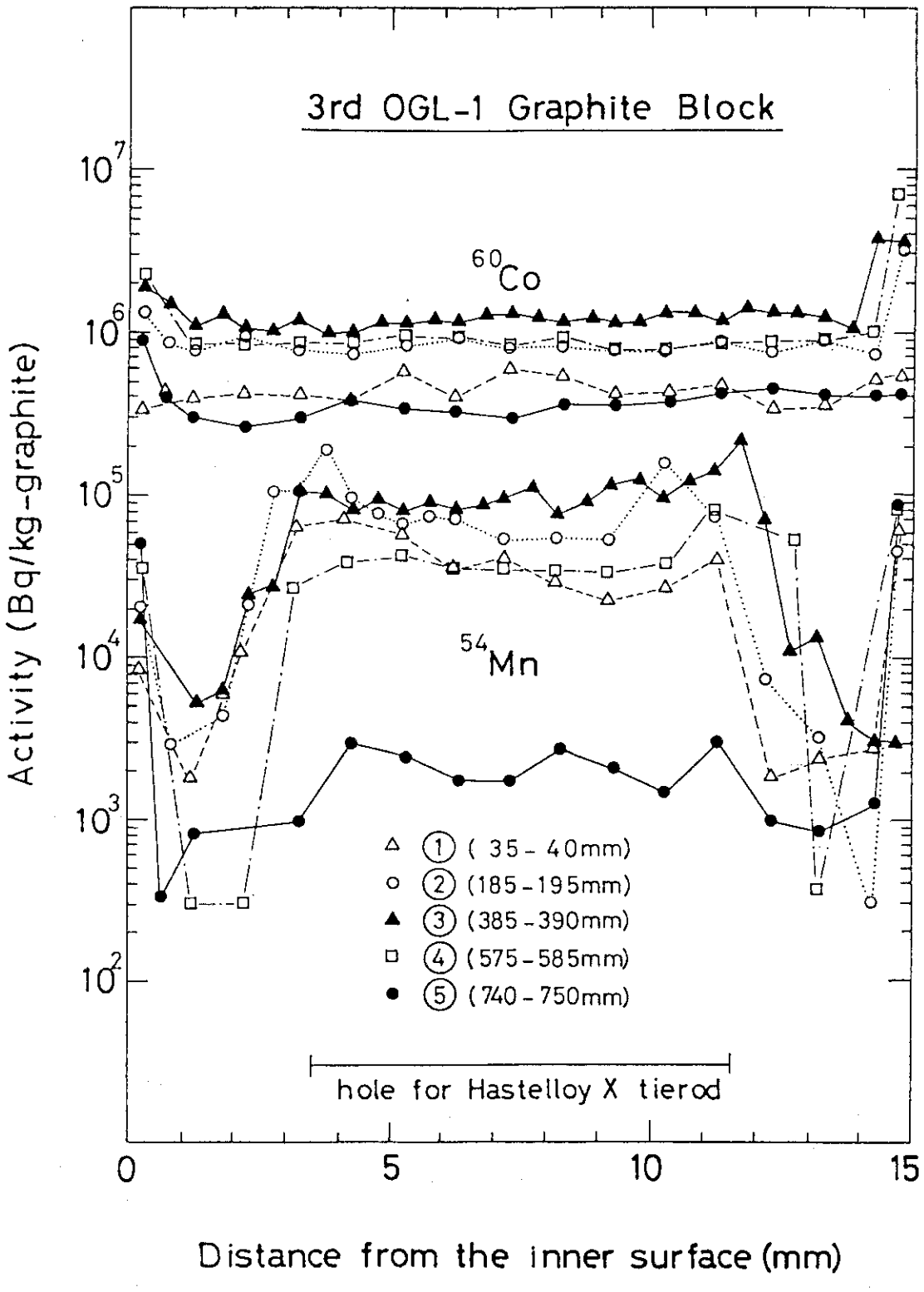

Fig.8 Radial profiles of ^{60}Co and ^{54}Mn at different axial positions of the graphite block of the third OGL-1 fuel assembly.

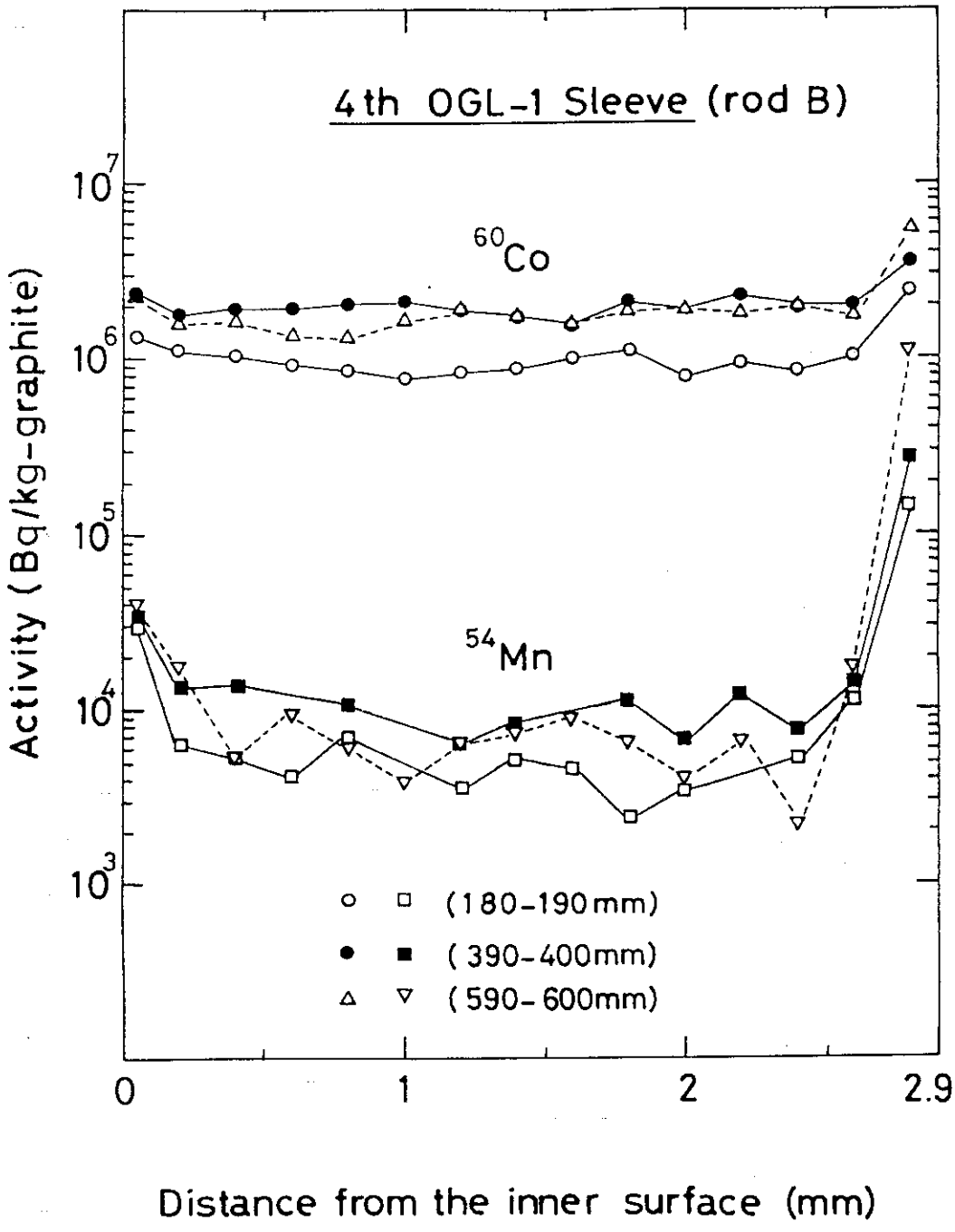

Fig.9 Radial profiles of ^{60}Co and ^{54}Mn at different axial positions of the fourth OGL-1 fuel sleeve.